Submitted to the Astrophysical Journal Supplement

Cosmic Chronometers: Constraining the Equation of State of Dark Energy. II. A Spectroscopic Catalog of Red Galaxies in Galaxy Clusters

Daniel Stern[1], Raul Jimenez[2], Licia Verde[2], S. Adam Stanford[3], Marc Kamionkowski[4]

ABSTRACT

We present a spectroscopic catalog of (mostly) red galaxies in 24 galaxy clusters in the redshift range $0.17 < z < 0.92$ obtained with the LRIS instrument on the Keck I telescope. Here we describe the observations and the galaxy spectra, including the discovery of three cD galaxies with LINER emission spectra, and the spectroscopic discovery of four new galaxy-galaxy lenses in cluster environments.

Subject headings: cosmology: observation

1. Introduction

The nature of the physics driving cosmic acceleration is perhaps the biggest question facing physics today. Huge resources and large collaborations are now being amassed to determine the dark-energy equation-of-state parameter $w \equiv p/\rho$, relating the cosmic pressure p to the energy density ρ (in units of $c \equiv 1$). The value of w could either be constant, as in the case of a cosmological constant ($w = -1$), or time-dependent, as in the case of a rolling scale field or "quintessence" (Peebles & Ratra 1988; Caldwell et al. 1998). Any such behavior would have far-reaching implications for particle physics. The avenues that are now receiving the most attention are supernova searches, weak lensing, baryon acoustic oscillations, and cluster counts. However, none of these will be free from systematics, and it is still not clear which is the most promising approach. Most likely, multiple approaches will be required, and new ideas still need to be explored.

A new approach, proposed by Jimenez & Loeb (2002), is to measure the relative ages of luminous red galaxies, a probe that is particularly sensitive to the *variation* of $w(z)$ with redshift

[1]Jet Propulsion Laboratory, California Institute of Technology, 4800 Oak Grove Drive, Mail Stop 169-506, Pasadena, CA 91109 [e-mail: stern@zwolfkinder.jpl.nasa.gov]

[2]ICREA & Institute of Sciences of the Cosmos (ICC), University of Barcelona, Barcelona 08028, Spain

[3]University of California, Davis, CA 95616 and Institute for Geophysics and Planetary Physics, Lawrence Livermore National Laboratory, Livermore, CA 94551

[4]California Institute of Technology, Mail Stop 350-17, Pasadena, CA 91125

z. This method was demonstrated to work in Jimenez et al. (2003) with a set of low-redshift ($z \lesssim 0.25$) Sloan Digital Sky Survey (SDSS) luminous red galaxies from the sample of Eisenstein et al. (2001) supplemented with approximately two dozen moderate-redshift ($z \lesssim 1$) early-type galaxies observed with Keck. That work found $w \leq -0.8$ at the 68% confidence level. Using the SDSS sample to measure dz/dt at $z \sim 0$, that work also derived an independent estimate for the Hubble constant, $H_0 = 69 \pm 12\,\mathrm{km\,s^{-1}\,Mpc^{-1}}$. Although this new cosmological test faces challenges from astrophysical uncertainties, these are not necessarily any more daunting than those associated with the more classical dark energy probes.

We describe here the results of a several night experiment with the Keck I telescope to obtain spectra of early-type galaxies in clusters at $0.2 \lesssim z \lesssim 1$. As demonstrated in Treu et al. (2005), the most massive early-type galaxies have the highest formation redshifts and are thus best suited to this experiment. Such galaxies are concentrated in galaxy clusters, with the additional benefit that *GALEX* observations show that cluster elliptical galaxies have less UV emission than field elliptical galaxies (e.g., Schawinkski et al. 2007). This implies that cluster ellipticals have the lower levels of "frosting" by recent star formation and thus are best suited for this experiment.

The multiplexing and unparalleled blue sensitivity of the Low Resolution Imaging Spectrometer (LRIS; Oke et al. 1995) on the Keck I telescope is a crucial aspect of this project, allowing simultaneous and accurate spectrophotometry of up to 20 cluster galaxies over a very wide spectral range, probing down to 2000 Å in the restframe. The importance of the UV stellar breaks at restframe 2640 Å and 2900 Å (B2640, B2900) was shown by Fanelli et al. (1992) and were used by Dunlop et al. (1996) and Spinrad et al. (1997) to determine the age of the high-redshift, quiescent radio galaxy LBDS 53W091. A comprehensive study by Dorman et al. (2003) dramatically shows that the restframe UV spectral region can be modeled accurately and, more importantly, that UV light (bluewards of the 4000 Å region) can help to break the age-metallicity degeneracy.

Stern et al. (2009, Paper I) presents the cosmological results from this experiment and the derived constraints on both the equation of state of dark energy and the value of the Hubble constant, H_0. This paper (Paper II) presents the data in some detail, including target selection, observing strategy, data processing (§2), and a catalog of approximately 500 sources in the fields of galaxy clusters out to $z \approx 1$ (§3.1). It is hoped that this resource will be useful for a number of other projects, such as more classic studies of galaxy and galaxy cluster evolution. In particular, we identified several interesting cD galaxies (§3.2) and we serendipitously found four new galaxy lenses (§3.3). Since most of the target sample are well-known clusters, some of these lenses already have *Hubble Space Telescope* imaging, and a more detailed analysis of the lens systems will be presented in Moustakas et al. (in prep.). During the course of this program, we also observed and derived the mass of a stellar black hole in the Virgo globular cluster RZ 2109 (Zepf et al. 2008).

2. Data

Nine nights were awarded for this experiment between February 2007 and September 2008 (Table 1). Unfortunately, five of the nights were completely lost to weather (four nights) or instrument problems (one night). In particular, our two night observing run in August 2007 was lost to a combination of Hurricane Flossie (category four), two earthquakes (magnitude 5.4 and 4.0), and a tsunami warning (due to a magnitude 8.0 earthquake in Peru). Of the four dedicated nights during which we obtained data, two (in December 2007) suffered from both a bright ($> 50\%$) moon and poor conditions (thick cirrus and $\gtrsim 1\farcs5$ seeing). As shown in Table 1, we obtained a handful of additional observations during nights dedicated to other programs.

2.1. Target Selection

We targeted rich galaxy clusters in order to obtain an as large as possible sample of red galaxies over the redshift range $0.2 < z < 1$. Most of the clusters are well-known, rich X-ray clusters from a variety of samples such as the Abell (1958) catalog, the *ROSAT* Cluster Survey (RCS; Rosati et al. 1998) and the Massive Cluster Survey (MACS; Ebeling et al. 2001). In the redshift range $0.5 < z < 1$, fewer rich X-ray clusters are known, so we targeted (and confirmed) two of the richest *Spitzer* mid-infrared selected cluster candidates from the IRAC Shallow Cluster Survey (Eisenhardt et al. 2008). Many of the targeted clusters were also observed in the near-infrared cluster survey of Stanford et al. (2002), which provided a valuable and consistent astrometric resource for slitmask designs. The list of clusters targeted is presented in Table 2.

The galaxy cluster sample was chosen to meet the competing demands of providing a good distribution of cluster redshifts for the cosmological experiment, a good right ascension distribution for the assigned nights, as well as a good right ascension distribution of brighter clusters to observe during poor conditions. Once a cluster was chosen for observation, selecting early-type galaxy cluster members with which to fill the slitmasks was an intensive process. We relied heavily on the NASA/IPAC Extragalactic Database (NED) to identify cluster members in the literature. For many clusters, we were able to spectroscopically target known cluster members that had no known signatures of star formation or AGN activity. Some clusters also had published lists of candidate cluster members based on either morphology or red colors from the optical to the near-infrared (e.g., Stanford et al. 2002). For the Boötes clusters in the IRAC Shallow Survey (Eisenhardt et al. 2004; Ashby et al. 2009), photometric redshifts based on optical thru mid-infrared data were used to select candidate early-type cluster members (Brodwin et al. 2006). Many of the clusters also had publicly available images in the *Hubble Space Telescope* archive from which we were able to morphologically and/or color select candidate cluster members.

One challenge of the myriad source lists used to populate the masks was that each source list was based on a slightly different astrometric reference frame. For the mask design, we required consistent astrometry for all candidates across the full $5' \times 7'$ LRIS field, including a minimum

of three alignment stars brighter than $B \sim 20$. For the lower redshift clusters, publicly available images from the Palomar Sky Survey or SDSS proved sufficient. For the higher redshift clusters, however, candidate cluster members were often too faint to provide robust centroiding in those shallow data. For most of these clusters we obtained images with the roboticized Palomar 60″ (P60) telescope (Cenko et al. 2006) which is equiped with a SITe 2048 × 2048 pixel CCD with a pixel scale of 0.″378 pixel^{-1} and a 12.′9 × 12.′9 field of view. For each cluster, we observed two bands chosen to straddle the 4000 Å break (D4000) at the cluster redshift. These multi-band images, either from the P60 or the public data sets, provided an additional sample of red sources near the cluster with which to populate the masks. Note that due to the geometric contraints from the mask designs, masks inevitably including a few targets which were unlikely to be cluster members.

2.2. Observing Strategy

The key goal of this program was to provide high signal-to-noise ratio, wide wavelength coverage spectroscopy of a large number of early-type galaxies at moderate redshifts. These spectra were then modeled to derive the ages of the galaxy stellar populations. Since restframe UV light probes the youngest, most massive stars in a galaxy, blue sensitivity is crucial for this experiment. Of all the optical spectrographs on 8 - 10 m class telescopes currently available, LRIS on the Keck I telescope is unique in being the only dual-beam spectrograph, thus providing sensitive observations across the entire optical window ($\lambda \sim 3200$ Å $- 1$ μm).

LRIS provides spectra of approximately 25 sources simultaneously across a $\sim 5' \times 7'$ field of view, with a dichroic splitting the light between the blue and red channels. For most of the observations, we observed the same mask with two different dichroics, thereby ensuring that the final spectra have no gaps which might compromise the stellar population modeling. Only the three masks observed in February 2005 were observed with a single dichroic. LRIS has an ample set of dichroics to choose from; we consistently selected dichroics that avoided the rest-frame 4000 Å spectral region which includes import stellar population diagnostics (e.g., [O II] λ3727, D4000 and the Balmer break).

We obtained the blue channel data with the 400 lines mm^{-1} grism, which has a central wavelength of 3400 Å and a spectral range of 4450 Å. We obtained the red channel data with the 400 lines mm^{-1} grating, which has a central wavelength of 8500 Å and a spectral range of 3800 Å. Combining the blue and red channel data from the two dichroic settings, sources typically had final spectra which spanned the entire ~ 3200 Å -1 μm optical window, albeit with higher noise at the short and long wavelength extremes. Based on analysis of sky lines, sources filling the 1.″5 wide slitlets used for these observations have resolution $\lambda/\Delta\lambda \sim 500$ and ~ 650 for the blue and red channels, respectively. Standard stars from Massey & Gronwall (1990) were observed with the same instrument configuration for the purposes of spectrophotometric calibration.

Observations were generally obtained with two dithered exposures per dichroic configuration with typical integration times of 900 s to 1800 s, depending on the cluster redshift and observing conditions. This allowed both improved cosmic ray rejection and, by pair-wise subtraction of the red images, removal of the fringing which strongly affects the long wavelength ($\lambda \gtrsim 7200$ Å) LRIS data. This required minimum slitlet lengths of approximately $10''$. Since LRIS has an atmospheric dispersion corrector, mask position angles were optimized based on the cluster orientation and no special attention was necessary to align the masks with the parallactic angle.

2.3. Reductions

We processed the spectroscopic data with `BOGUS`[5], which is an IRAF routine designed for two-dimensional processing of multislit data and was written by D. Stern, A. Bunker, and S. A. Stanford. After gain and overscan correction of the raw two-dimensional images, `BOGUS` basically splits the mask into individual slitlets and processes each slitlet using standard optical longslit techniques. After flattening the spectrum with either domeflats (recommended for the red channel of LRIS) or twilight flats (recommended for the blue channel of LRIS), cosmic rays are identified from unsharp masking of the images, sky lines are subtracted using a low order polynomial fit to each column, and images are shifted by integer pixels in the spatial and dispersion directions and recombined. For the red channel data, an additional step of pair-wise image subtraction improves fringe subtraction at long wavelength. As a final step, `BOGUS` shifts each of the slitlets to roughly align them in the wavelength direction. This both simplifies wavelength calibration and the rapid visual identification of spectroscopically-confirmed cluster members.

After the two-dimensional processing provided by `BOGUS`, we extracted the spectra using $1\farcs5$ wide extraction traces using the `APALL` procedure within IRAF. We extracted arc lamps in an identical manner and used them to do a first pass wavelength calibration of the data. This typically relied on a fourth order polynomial wavelength solution, providing a ≈ 0.5 Å RMS to the blue channel of LRIS and a ≈ 0.1 Å RMS to the red channel of LRIS. As a final step in the wavelength calibration, these lines were linearly shifted based on the sky lines and we conservatively estimate that the wavelength solutions are robust to better than 1 Å. We flux calibrated the spectra using spectrophotometic standards observed during each observing run.

At this point, each slitmask target generally has four spectra: the blue and red channel observations for each of the two dichroics. To combine the spectra into a single, final spectrum for the stellar population synthesis analysis, we did the following. Spectra were trimmed at their blue and red ends to restrict coverage to regions of more robust spectrophotometry. Generally, wavelengths blueward of observed ~ 3500 Å were removed due to their lower signal-to-noise. Pixels within 50 Å of the dichroics were eliminated. At long wavelength, spectral trimming depended on individual

[5]Available upon request from the first author.

analysis of the spectra. Fainter targets and/or targets observed with no dithering often showed significant systematic glitches in their long wavelength data, and thus were trimmed at relatively blue wavelengths ($\sim$ 7500 Å). Other sources had robust spectra out to $\sim$ 9500 Å. Since the observations were not all obtained in photometric conditions, the final combination of the spectra required multiplicative scaling of their calibrated spectra, which generally was normalized to the blue channel data with the longer wavelength dichroic. We derived statistical error spectra assuming Poisson uncertainties of sky plus science target counts within the extraction regions. For observations where an extra step of fringe subtraction was applied, the error spectra were increased by $\sqrt{2}$ to account for the statistical noise hit from that procedure. During the final step of combining the multiple spectra (which generally were all obtained with the same exposure time), the error spectra were averaged and scaled down by $\sqrt{2}$.

3. Results

3.1. Spectra of Galaxies in Clusters

Figure 1 presents the results from the a typical mask: MACS J0159.8−0849 at $z = 0.405$, observed on UT 2008 September 3. Nearly 20 early-type cluster members were obtained simultaneously, each clearly showing an evolved stellar population with strong Ca H and K absorption and a prominent D4000 break. Figure 2 averages spectra of cluster members for masks observed in late 2008 and shows a clear sequence with redshift: clusters at lower redshift contain older stellar populations, recognized from their redder spectral energy distributions (SEDs) and larger D4000 breaks.

Table 3 presents the results from the spectroscopy. The spectra are classified both on the basis of their quality and their spectral class. Quality "A" indicates very reliable redshifts, generally based on multiple, well-observed features. Quality "B" indicates reliable redshifts, but often based on a single feature — e.g., a single emission line is observed and is assumed to be either Lyα or [O II], or a break is identified, but not with sufficient fidelity to derive a precision redshift. Such redshifts are likely correct, though an occasional misidentification is possible. Based on a comparison of redshifts derived from multiple features, quality "A" redshifts are conservatively estimated to have uncertainties of 0.002 in redshift. Assuming the features are correctly identified, quality "B" emission line redshifts will have comparable uncertainties, while quality "B" absorption line redshifts will have uncertainties twice as large. Our internal processing also included quality "C" (tentative) and "F" (uncertain) flags; such sources are omitted from Table 3.

We assign each of the spectra one of four spectroscopic classes (or a hybrid of these classes). Spectroscopic class "E" refers to early-type or elliptical galaxy spectra, showing only spectral breaks and absorption lines. Such sources were the primary goal of this program. Spectral class "S" refers to late-type or spiral galaxy spectra, showing emission lines such as [O II], Hβ, [O III] and Hα, typical of star forming galaxies. We identified several stars during this program, tabulated as

spectral class "⋆". Many are late-type stars of spectral class M, mistakenly targeted on the basis of their red colors mimicing that of moderate-redshift early-type galaxies. A handful of early-type stars were also serendipitously observed. Finally, we observed a handful of active galaxies, listed as spectral class "AGN."

In total, we obtained 496 redshifts in galaxy cluster fields during this program, of which the vast majority (464, or 94%) are quality "A" (Figure 3). For the targeted cluster early-type galaxy sample, we obtained a total of 278 sources, of which 260 are quality "A." Note that just because a source is of quality "A" doesn't ensure that it will be useful for the cosmic chronometer experiment. A target might have a reliable redshift due to the detection of specific features, while the continuum might be of low signal-to-noise ratio due to poor fringe subtraction, contamination from a nearby source, or simply due to the observing conditions. Stern et al. (2009) analyzes this sample, deriving stellar population ages by modeling the spectra.

3.2. cD Galaxies

Three of the central cD galaxies observed during this program have interesting spectra showing multiple emisison lines superposed on a red, evolved stellar population (Figure 4). The spectra are similar to that of NGC 1275, the central galaxy in the Perseus cluster (e.g., Sabra et al. 2000), and are clearly classified as LINER-like spectra. Indeed, log ([O I] 6300/[O III] 5007) ranges from 0.13 to 0.59 for the three galaxies, which is much larger than typical of star-forming galaxies in the SDSS (Brinchmann et al. 2008). All three galaxies are detected by the Faint Images of the Radio Sky at Twenty cm survey (FIRST; Becker et al. 1995), with 1.4 GHz flux densities of 31.43 mJy, 5.59 mJy and 16.75 mJy for MACS J015949.3−84958, MACS J162124.7+381008 and MACS J172016.7+353626, respectively.

While typically only a modest fraction ($\approx$ 15%) of brightest cluster galaxies (BCGs) show strong optical line emission, optical line emission is quite common (71^{+9}_{-14}%) for BGCs in cooling flow clusters (Edwards et al. 2007). The line emission is presumed related to the cooling of X-ray gas at the cluster center. For the well-studied, local example of NGC 1275, the line emission is concentrated in a spectacular network of filaments extending over several arcminutes. The filaments are thought due to compressed, cooling intracluster gas within a relativistic plasma ejected by the active nucleus of NGC 1275 (Conselice et al. 2001). NGC 1275 also shows evidence of recent star formation. Understanding such systems in detail is likely important for probing the physics of feedback in massive galaxies.

3.3. Lensed Galaxies

Four of the cluster galaxies observed as part of this program show additional emission lines at blue wavelengths superposed on cluster early-type spectra. These emission lines are spatially

extended in three of the four sources (Figure 5). In all four sources the emission lines do not match the absorption line redshift (Figure 6). The spectra are reminiscent of lenses spectroscopically identified in the SDSS luminous red galaxy sample, such as the $z = 2.7$ Einstein cross identified by Bolton et al. (2006b) and lower redshift strong lenses identified by the Sloan Lens ACS (SLACS) survey (Bolton et al. 2006a). Two of the four new lenses have publicly available, two-band Advanced Camera for Surveys (ACS) images in the *Hubble* Legacy Archive. These images, presented in Figure 7, clearly show strongly lensed background galaxies behind red, early-type galaxies. Such systems are valuable probes of the lensing galaxy mass and mass profile. Moustakas et al. (in prep.) presents a detailed analysis of these new systems.

4. Summary

We present a catalog of nearly 500 redshifts obtained in the fields of 24 galaxy clusters, including nearly 300 early-type cluster members. Paper I derives ages for this sample and uses their ages to probe cosmological parameters using the differential age or cosmic chronometer test. This database will also be useful for studying the properties of galaxy clusters, modeling their mass distributions, and understanding the formation mechanism of both clusters and the constituent galaxy populations. We identify three interesting central galaxies showing strong, LINER-like spectra, typical of cooling flow clusters. We also serendipitously identify four new galaxy-galaxy lenses on the outskirts of galaxy clusters.

The authors wish to recognize and acknowledge the very significant cultural role and reverence that the summit of Mauna Kea has always had within the indigenous Hawaiian community; we are most fortunate to have the opportunity to conduct observations from this mountain. We thank M. Kasliwal for assistance with the P60 scheduling, and F. Harrison and R. Griffith for assisting with the March 2009 Keck observations. We also thank A. Barth for an interesting discussion of the cD galaxy spectra. The work of DS was carried out at Jet Propulsion Laboratory, California Institute of Technology, under a contract with NASA. RJ and LV acknowledge support from the Spanish Ministerio de Ciencia e Innovacion and the European Union FP7 program. MK was supported by DoE DE-FG03-92-ER40701 and the Gordon and Betty Moore Foundation. This research made use of the NASA/IPAC Extragalactic Database (NED) which is operated by the Jet Propulsion Laboratory, California Institute of Technology, under contract with NASA. Figure 7 is based on observations made with the NASA/ESA *Hubble Space Telescope*, and obtained from the *Hubble* Legacy Archive, which is a collaboration between the Space Telescope Science Institute (STScI/NASA), the Space Telescope European Coordinating Facility (ST-ECF/ESA) and the Canadian Astronomy Data Centre (CADC/NRC/CSA).

References

Abell, G. O. 1958, ApJS, 3, 211

Ashby, M. L. N., Stern, D., Brodwin, M., Griffith, R., Eisenhardt, P., et al. 2009, ApJ, in press (astro-ph/0906.0024)

Becker, R. H., White, R. L., & Helfand, D. J. 1995, ApJ, 450, 559

Bolton, A. S., Burles, S., Koopmans, L. V. E., Treu, T., & Moustakas, L. A. 2006a, ApJ, 638, 703

Bolton, A. S., Moustakas, L. A., Stern, D., Burles, S., Dey, A., & Spinrad, H. 2006b, ApJ, 646, L45

Brinchmann, J., Kunth, D., & Durrett, F. 2008, A&A, 485, 657

Brodwin, M. et al. 2006, ApJ, 651, 791

Caldwell, R., Davé, R., & Steinhardt, P. 1998, Phys. Rev. Lett., 80, 1582

Cenko, S. B. et al. 2006, PASP, 118, 1396

Conselice, C. J., Gallagher III, J. S., & Wyse, R. F. G. 2001, AJ, 122, 2281

Dorman, B., O'Connell, R. W., & Rood, R. T. 2003, ApJ, 591, 878

Dunlop, J. S., Peacock, J. A., Spinrad, H., Dey, A., Jimenez, R., Stern, D., & Windhorst, R. A. 1996, Nature, 381, 581

Ebeling, H., Edge, A. C., & Henry, J. P. 2001, ApJ, 553, 668

Edwards, L. O. V., Hudson, M. J., Balogh, M. L., & Smith, R. J. 2007, MNRAS, 379, 100

Eisenhardt, P. R. et al. 2004, ApJS, 154, 48

—. 2008, ApJ, 684, 905

Eisenstein, D. J. et al. 2001, AJ, 122, 2267

Fanelli, M. N., O'Connell, R. W., Burstein, D., & Wu, C. C. 1992, ApJS, 82, 197

Jimenez, R. & Loeb, A. 2002, ApJ, 573, 37

Jimenez, R., Verde, L., Treu, T., & Stern, D. 2003, ApJ, 593, 622

Massey, P. & Gronwall, C. 1990, ApJ, 358, 344

Oke, J. B., Cohen, J. G., Carr, M., Cromer, J., Dingizian, A., Harris, F. H., Labrecque, S., Lucinio, R., Schaal, W., Epps, H., & Miller, J. 1995, PASP, 107, 375

Peebles, P. J. E. & Ratra, B. 1988, ApJ, 435, L17

Rosati, P., della Ceca, R., Norman, C., & Giacconi, R. 1998, ApJ, 492, L21

Sabra, B. M., Shields, J. C., & Filippenko, A. V. 2000, ApJ, 545, 157

Schawinkski, K. et al. 2007, ApJS, 173, 512

Spinrad, H., Dey, A., Stern, D., Peacock, J. A., Dunlop, J., Jimenez, R., & Windhorst, R. A. 1997, ApJ, 484, 581

Stanford, S. A., Holden, B., Rosati, P., Eisenhardt, P. R. M., Stern, D., Squires, G., & Spinrad, H. 2002, AJ, 123, 619

Stern, D., Jimenez, R., Verde, L., Kamionkowski, M., & Stanford, S. A. 2009, JCAP, submitted (astro-ph/0907.3149)

Treu, T., Ellis, R. S., Liao, T. X., van Dokkum, P. G., Tozzi, P., Coil, A., Newman, J., Cooper, M. C., & Davis, M. 2005, ApJ, 633, 174

Zepf, S. E., Stern, D., Maccarone, T. J., Kundu, A., Kamionkowski, M., Rhode, K. L., Salzer, J. J., Ciardullo, R., & Gronwall, C. 2008, ApJ, 683, L139

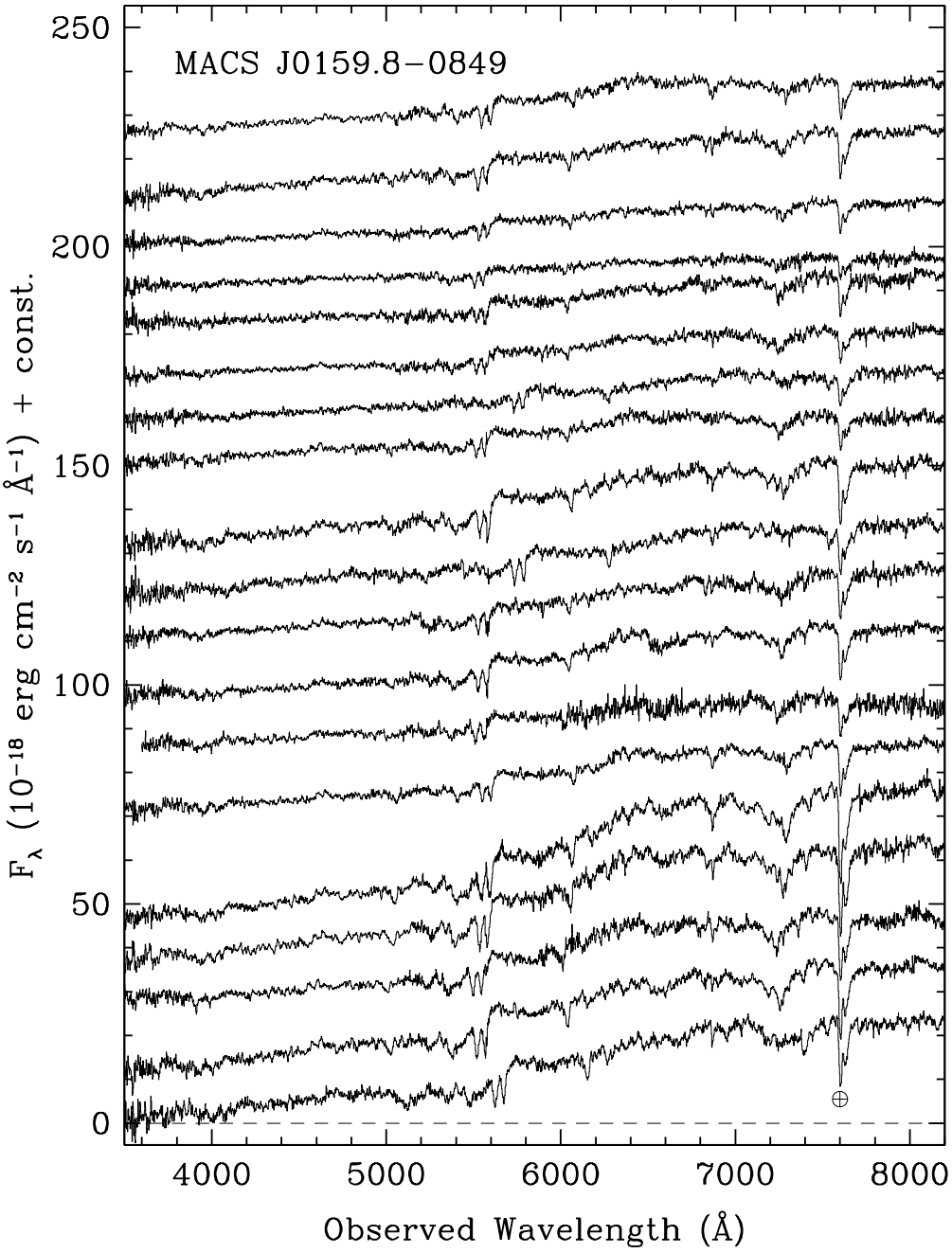

Fig. 1.— Results of a typical mask, MACS J0159.8−0849 at $z = 0.405$, observed on UT 2008 September 3. Telluric A-band absorption is indicated.

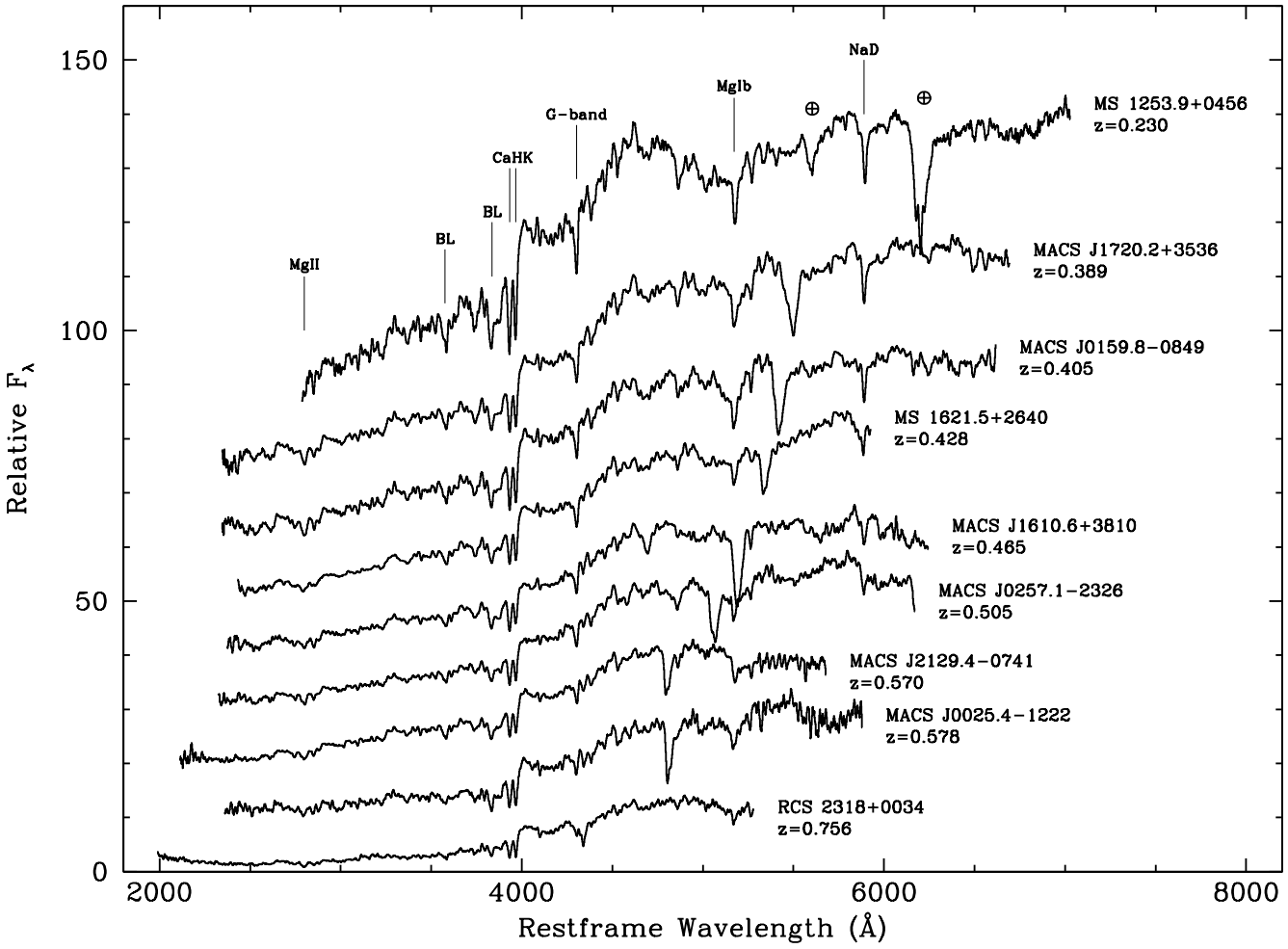

Fig. 2.— Averaged spectra of cluster ellipticals from the observing runs in July and September 2008, plotted as a function of redshift. Primary spectral features are indicated. Telluric A-band (7600 Å) and B-band (6880 Å) absorption are indicated for the lowest redshift cluster (top); these features shift to shorter restframe wavelengths for the higher redshift clusters.

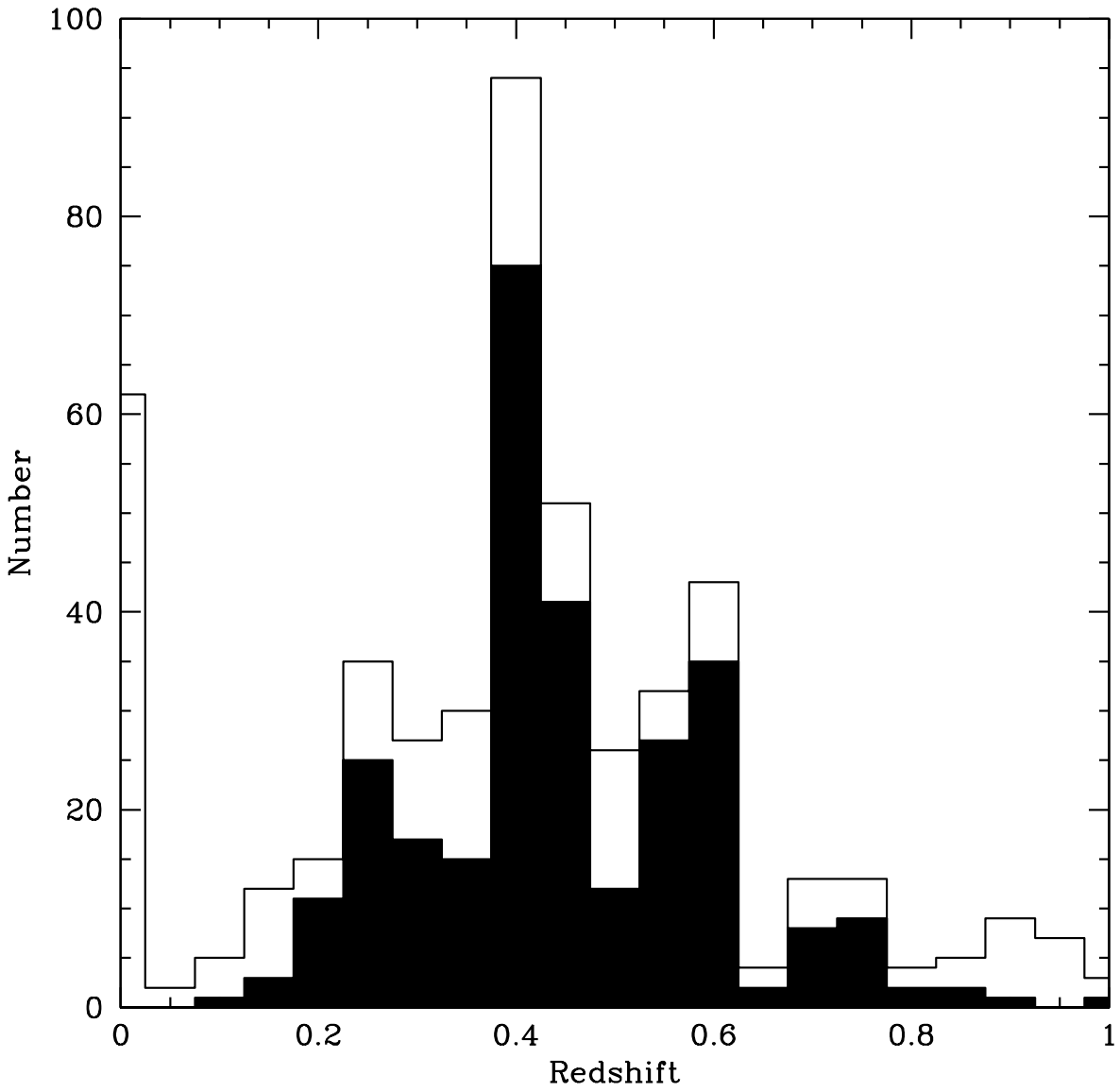

Fig. 3.— Histogram of redshifts derived from this program. The open histogram shows all 496 sources, while the solid histogram only shows the highest quality (quality "A") absorption-line (class "E") redshifts. Note the high fraction of early-type galaxies from this program, much higher than would be found in a field galaxy survey.

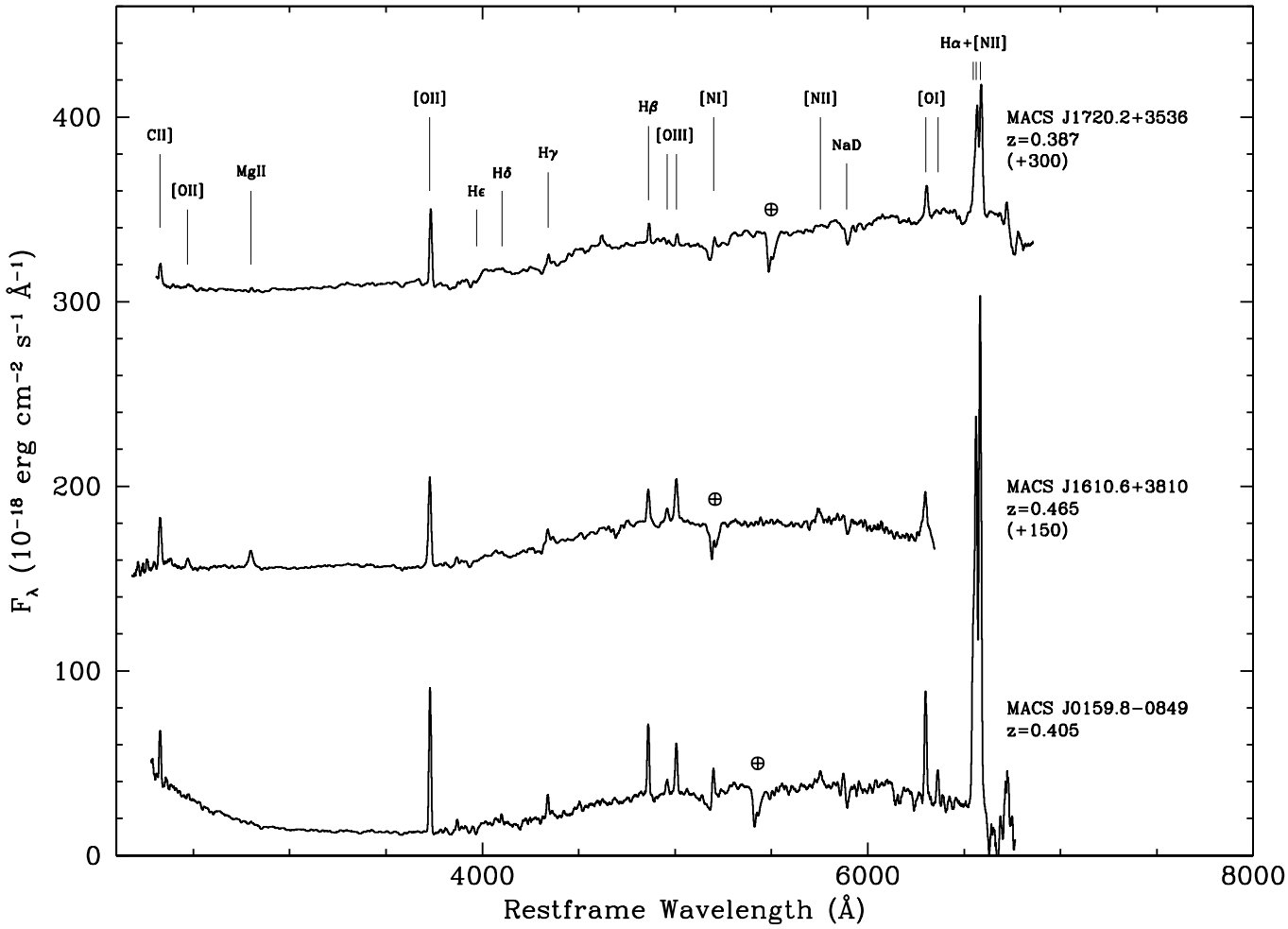

Fig. 4.— Spectra of three cluster cD galaxies showing strong emission lines, typical of LINERs.

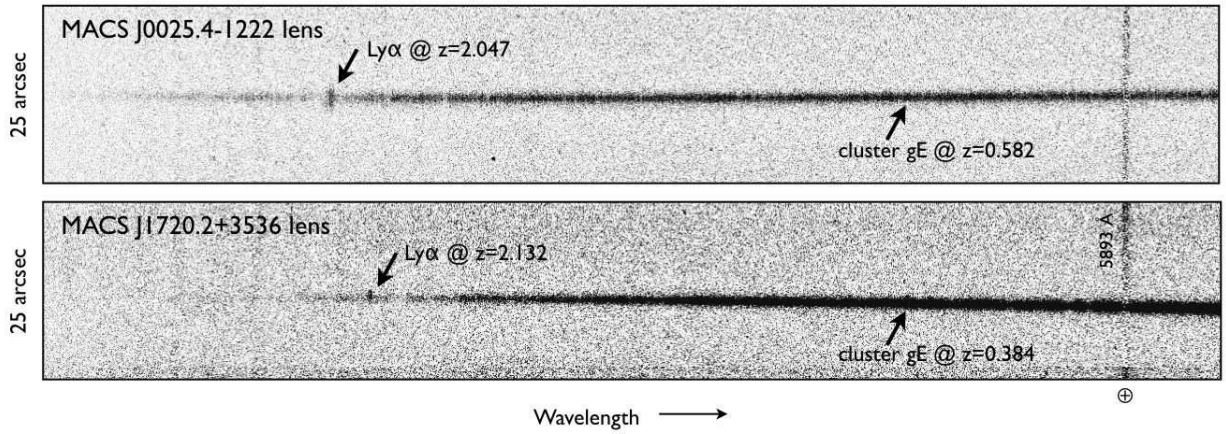

Fig. 5.— Two-dimensional processed spectra of two of the newly identified galaxy-galaxy lenses in cluster environments. Both images, obtained with the D680 grating and the blue channel of LRIS, span approximately from 2900 Å to 6150 Å in the dispersion (horizontal) axis and 25″ in the spatial (vertical) axis. Residuals from telluric NaD 5893 Å emission are visible at the long wavelength ends of the spectra. Both spectra show strong, extended Lyα emission superposed atop red emission from early-type members of the targeted MACS clusters.

Table 1. Cosmic Chronometer Observing Runs.

UT Date	% Dark	PI	Conditions/Comments
2005 Feb 10	94	Stanford	
2007 Feb 17-18‡	100	Kamionkowski	weathered out
2007 Aug 15-16‡	92-87	Kamionkowski	Hurricane Flossie, two earthquakes, tsunami warning
2007 Dec 17-18‡	48-40	Kamionkowski	poor conditions and bright moon
2008 Jul 1‡	89	Kamionkowski	
2008 Sep 2-3‡	93-87	Kamionkowski	1st night lost to mechanical problems
2009 Mar 2-3	62-52	Harrison	poor conditions and bright moon

Note. — ‡: Nights dedicated to cosmic chronometer experiment. Note the poor track record for the dedicated nights with only two successful nights out of nine allocations, thus traumatizing the PI during his first foray into observational astrophysics. Other observations were generally just a mask or two observed during nights focused on other programs.

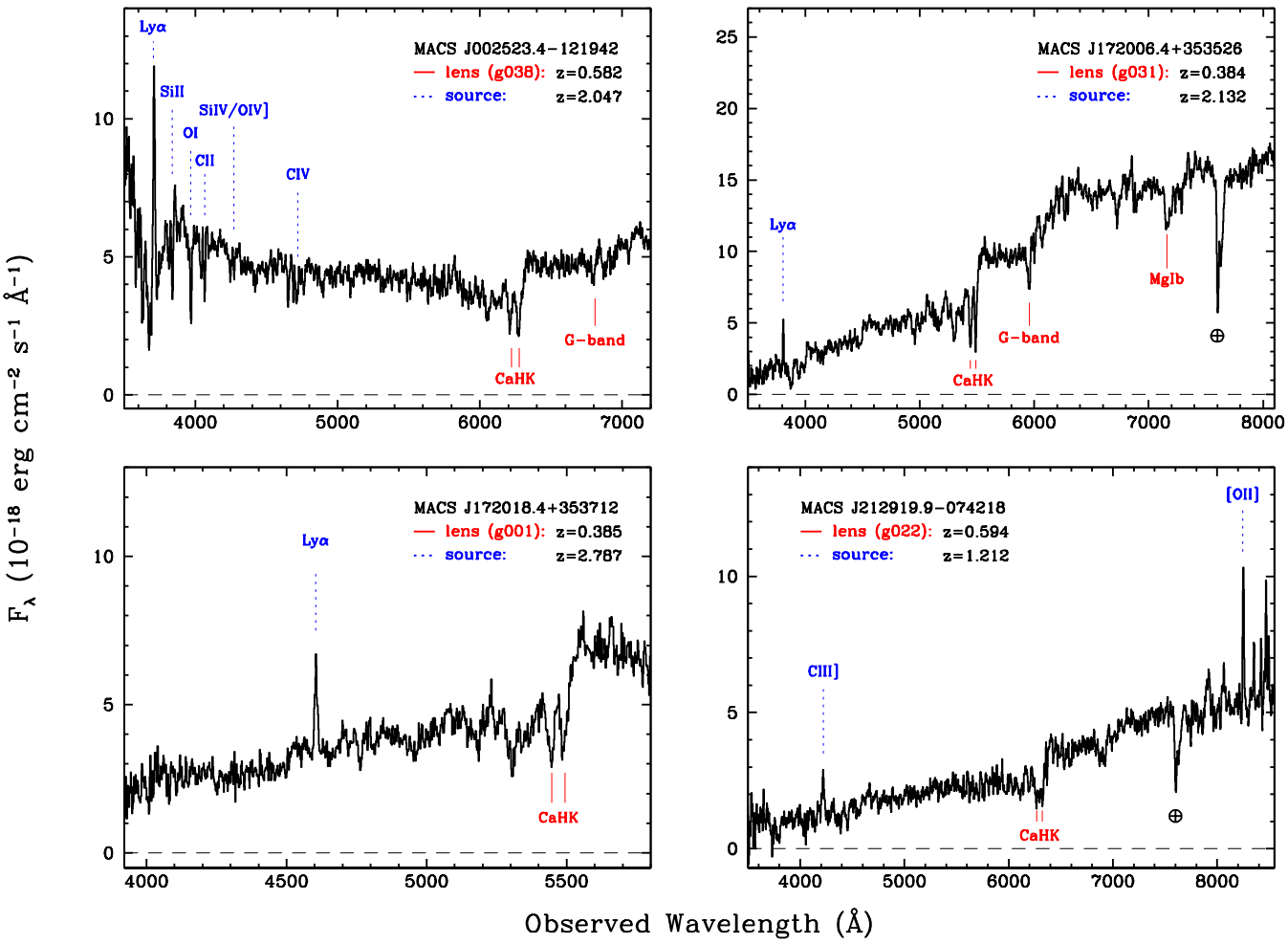

Fig. 6.— Extracted spectra of the four newly identified galaxy-galaxy lenses in cluster environments.

Fig. 7.— *HST*/ACS images of two of the newly identified galaxy-galaxy lenses in cluster environments. Both images, obtained from the *Hubble* Legacy Archive, are false color images created from F555W and F814W observations. Images are approximately 6″ on a side, with North up and East to the left.

Table 2. Galaxy Clusters Observed.

Galaxy Cluster	RA	Dec	Redshift	UT Date	PA (deg)	Comments
MS 0906.5+1110	09:09:12.7	+10:58:29	0.172	2005 Feb 10	−70.1	
MS 1253.9+0456	12:56:00.0	+04:40:00	0.230	2008 Jul 1	42.7	
Abell 1525	12:21:57.8	−01:08:03	0.260	2007 Dec 18	122.6	
MS 1008.1−1224	10:10:32.3	−12:39:52	0.301	2007 Dec 17	115.5	
CL 2244−0205	22:47:13.1	−02:05:39	0.330	2007 Dec 17-18	−124.4	poor conditions
Abell 370	02:39:53.8	−01:34:24	0.374	2007 Dec 18	70.0	
MACS J1720.2+3536	17:20:12.0	+35:36:00	0.389	2008 Sep 3	69.6	
CL 0024+16	00:26:35.7	+17:09:45	0.394	2007 Dec 18	−5.5	
MACS J0429.6−0253	04:29:41.1	−02:53:33	0.400	2008 Sep 3	46.3	
MACS J0159.8−0849	01:59:00.0	−08:49:00	0.405	2008 Sep 3	17.6	
Abell 851	09:43:02.7	+46:58:37	0.405	2007 Dec 17	60.3	
GHO 0303+1706	03:06:19.1	+17:18:49	0.423	2005 Feb 10	−60.0	
MS 1621.5+2640	16:23:00.0	+26:33:00	0.428	2008 Jul 1	27.9	
MACS J1610.6+3810	16:21:24.8	+38:10:09	0.465	2008 Sep 3	−47.1	
MACS J0257.1−2325	02:57:09.1	−23:26:06	0.505	2008 Sep 3	51.8	
MS 0451.6−0306	04:54:10.8	−03:00:57	0.539	2005 Feb 10	−39.1	
MS 0451.6−0306	04:54:10.8	−03:00:57	0.539	2007 Dec 17-18	−83.4	
Boötes 10.1	14:32:06.0	+34:16:47	0.544	2008 Sep 3	54.5	
CL 0016+16	00:18:33.5	+16:25:15	0.545	2007 Dec 18	139.4	very poor
MACS J2129.4−0741	21:26:46.9	−07:54:36	0.570	2008 Jul 1	75.0	
MACS J0025.4−1222	00:25:09.4	−12:22:37	0.578	2008 Jul 1	−25.9	
MACS J0647.7+7015	06:47:50.5	+70:14:55	0.591	2009 Mar 2	−71.1	mask 1
MACS J0647.7+7015	06:47:50.5	+70:14:55	0.591	2009 Mar 3	−95.5	mask 2
MACS J0744.8+3927	07:44:52.5	+39:27:27	0.697	2009 Mar 2	91.7	mask 1
MACS J0744.8+3927	07:44:52.5	+39:27:27	0.697	2009 Mar 3	97.6	mask 2
RCS 2318+0034	23:18:31.5	+00:34:18	0.756	2008 Sep 3	−26.1	
Boötes 10.8	14:32:06.0	+34:16:47	0.921	2008 Jul 1	−25.0	

Note. — Cluster positions are in the J2000 coordinate system.

Table 3. Spectroscopic Results.

Object ID	RA	Dec	Redshift	Quality	Class	Notes
CL0024 gxy07	00:26:24.620	+17:13:33.510	0.246	A	S	[O II],Hα
CL0024 gxy26	00:26:25.420	+17:13:22.812	0.399	A	E	MgB
CL0024 g202p	00:26:26.029	+17:11:16.559	0.392	A	E+S	[O II],CaHK
CL0024 g215p	00:26:27.117	+17:12:26.082	0.398	A	E	CaHK
CL0024 gxy21	00:26:27.709	+17:13:49.797	0.395	A	S	[O II]
CL0024 g226p	00:26:27.956	+17:11:37.879	0.394	A	E	CaHK
CL0024 gxy06	00:26:28.381	+17:12:46.550	0.397	B	E	CaHK
CL0024 gxy04	00:26:31.029	+17:12:09.808	0.0	A	$\star$	M-star
CL0024 gxy03	00:26:31.392	+17:10:56.131	0.397	A	E	CaHK
CL0024 g334p	00:26:34.210	+17:10:09.844	0.387	A	E	CaHK
CL0024 g338p	00:26:34.348	+17:10:22.630	0.388	A	E	CaHK
CL0024 gxy08	00:26:34.626	+17:08:10.100	0.0	A	$\star$	M-star
CL0024 g353p	00:26:34.838	+17:09:19.273	0.398	A	E	CaHK
CL0024 g362p	00:26:35.018	+17:09:39.309	0.399	A	E	CaHK
CL0024 g363p	00:26:35.206	+17:09:49.238	0.389	A	E	CaHK
CL0024 g383p	00:26:36.140	+17:08:27.616	0.402	A	E	CaHK
CL0024 gxy02	00:26:36.250	+17:10:00.925	0.390	A	E	CaHK
CL0024 gxy09	00:26:37.313	+17:07:50.647	0.392	A	E	CaHK
CL0024 gxy10	00:26:38.418	+17:07:31.566	0.392	A	E	CaHK
CL0024 g458p	00:26:41.879	+17:10:45.495	0.390	A	E	CaHK

Note. — A sample from the full table is shown above; the full table of 496 sources is included in the on-line version of the paper. Positions are in the J2000 coordinate system. Typical redshift uncertainties are ± 0.002. Only quality "A" (very reliable) and "B" (reliable) redshifts are presented. Spectroscopic classes are E (elliptical, or early-type spectrum), S (spiral, or late-type spectrum), AGN (quasar), and $\star$ (Galactic star).